Journal of Computational Applied Mechanics 2024, 55(4): 617-635

DOI: 10.22059/JCAMECH.2024.374122.1007

RESEARCH PAPER

Coupled loading hygro-thermo-mechanical Effect on the stability of imperfect functionally graded sandwich plates

Fouzi Masmoudi [a, b], Abdelkader Tamrabet [c,d], Salah Refrafi [e], Nimer Ali Alselmi [f], Abderahmane Menasria [b, e], Abdelhakim Bouhadra [b, e *], Samir Benyoucef [b]

[a] *Department of Irrigation and Civil Engineering, Faculty of Technology, Echahid Hamma Lakhdar University, El Oued, 39000, Algeria.*

[b] *Material and Hydrology Laboratory, Civil Engineering Department, Faculty of Technology, Djillali Liabes University, Sidi Bel Abbes 22000, Algeria.*

[c] *Department of Civil Engineering, Faculty of Technology, University of Ferhat Abbas, Setif 19137, Algeria.*

[d] *Research Unit of Emerging Materials, University of Ferhat Abbas, Setif 19137, Algeria.*

[e] *Department of Civil Engineering, Faculty of Science and Technology, Abbes Laghrour University, Khenchela 40000, Algeria.*

[f] *Civil Engineering Department, College of Engineering, Jazan University, Saudi Arabia.*

Abstract

In this research study, the hygro-thermo-mechanical responses of simply supported porous FG sandwich plates resting on a variable elastic foundation are studied by mean of a new height order shear deformation theory. The present model satisfies the nullity conditions of the shear stresses on the upper and lower surfaces of the FG plate and without using shear correction factors. The distribution of the properties of the material through the thickness of the sandwich plate is assumed to have a distribution according to a function of the power law, while the core is assumed to be purely ceramic. The derivation of the stability equations is obtained based on the principle of virtual works. The hygro-thermal loading is considered to have a uniform, linear and non-linear variation across the thickness of the plate. To verify the accuracy of the current model, a comparison was made with other authors of the literature. The effects of the hygro-thermo-mechanical loading, the porosity, the parameters of the elastic foundation « kw and kg », the thickness ratio « a/h », the aspect ratio « a/b » and the material index « k » on the critical buckling load of the FG plate are examined.

Keywords: FG sandwich plate, hygro-thermo-mechanical load, porosity, variable elastic foundation, stability equations.

1. introduction

Sandwich structures are widely used in the aviation, aerospace, naval/marine, construction, transportation, and wind energy systems industries due to their exceptional qualities, which include high rigidity and low weight

* Corresponding author. Tel.: +966-55-466-4596;
E-mail address: nalselami@jazanu.edu.sa

furthermore One novel application of this material is to reinforce concrete used in bridges, as fiber reinforced polymer (FRP) materials improve steel's resistance to corrosion and lengthen the material's life cycle.[1]. Applications in aerospace to support high thermal barrier coating include engine parts, spaceship trusses, Seebeck generators, rocket nozzles (TiAl metal SiC ceramic), high temperature heat exchanger panels, Aerotech, diesel, and polyurethane pipe.[2]

However, the abrupt variation in material characteristics within the interfaces between the face sheets and the core can result in large interlaminar stresses inducing delamination, which is an important problem in classical sandwich structures. Furthermore, the difference in the values of thermal coefficients of the materials may induce residual stresses. In order to solve these issues, the design of sandwich plates introduces the idea of functionally graded material (FGM) FGM is a type of advanced composite material in which the mechanical characteristics progressively and continuously vary from one surface of the structure to the other. The application of such materials aids in improving bonding strength and removing mechanically and thermally generated stresses resulting from material property mismatch.

To study the different behaviours of the thick FG sandwich plate, many analytical models are proposed. studied the stability of the porous FG sandwich plate under thermal load using the theory of first order shear deformation (FSDT). Al-Osta. investigates wave propagation in porous FG sandwich plates subjected to both thermal and moisture variations. While the main focus is wave propagation, the formulation employs a novel FSDT approach that considers the presence of porosity. This makes it applicable to studies analyzing the stability of porous FG sandwich plates under thermal loads as well[3]. WAN et al. [4] based on a new mathematical method (Differential Quadrature Hierarchical Finite Element Method) investigate how reinforcing a special plate with carbon nanotubes (CNTs) and carbon fibres (CFs) increases its stability, vibration, and energy absorption under various conditions Hadjlaoui et al. studied the temperature-dependent material properties were considered to perform a thermal buckling analysis. The performance of the present formulation based on FSDT is demonstrated through comparisons with existing studies on the thermal buckling of FGM shells[5]. Mohammadi, M., et al investigated the effect of viscos- Pasternak foundation on the vibration behavior of the nanobeam subjected on hygrothermal environment based on the differential quadrature method. They founded that the result obtained maybe could be used to design design and manufacture various structures similar to nano sensors, biosensors [6]Mantari et Granados proposed a new shear deformation model based on indeterminate integral terms for the bending analysis of sandwich plates with FG core and isotropic skins[7]. Sobhy studied the stability and dynamic behavior of EFG sandwich plates with different types of foundations using the shear deformation theory with five variables[8]. Mohammadi, M. A. Farajpour, and M. Goodarzi used principal of virtual work to drive the governing equation of rectangular graphene sheet for the free vibration behavior under shear in-plane load, then they are solved it based on DQM and Galerkin methods. It found that the vibration frequencies are strongly dependent on the small scale coefficient Nguyen et al. have developed a high-order inverse tangential shear deformation theory to study the bending, buckling and free vibration of isotropic-core FG sandwich plate and FG skins and FG-core FG sandwich plate and isotropic skins[9]. Wave propagation of micro air vehicle wings with porous functionally graded materials (FGM) and magnetostrictive nanocomposite layers is studied by Al-Furjan et al.[10]based on new refined zigzag theory (RZT) and Halpin-Tsai material distribution model. Shan et al[11] present a review on the effect of various nanoparticles on the mechanical behavior of nanocomposites such as flexural, tensile, interlaminar shearing strength, impact, vibration, thermal properties, buckling and post-buckling, fatigue behavior, and recent advances in improving these mechanical characteristics. Mohammadi, M., et al investigated the effect of temperature change and elastic medium on the vibration behavior of annular and circular graphene sheet by employed Both Winkler and Pasternak foundation and they concluded that the non-dimensional frequency decreases at high temperature case with increasing the temperature change for all boundary conditions . Based on the HSDT, Chitour et al. employed a quasi-3D high-order theory to investigate the stability of functionally graded (FG) sandwich plates incorporating metallic foam cores. Their work, which is the first of its kind, explores how factors like gradient index, geometric properties, porosity distribution within the FG layers, and the metal foam itself affect the critical buckling load of these sandwich plates[12]. Mohammadi, M., et al analyzed the effect of porosity on the free and forced vibration of FG nanobeam under mechanical and electrical loads based on Hamilton's and Galerkin methods and they found that the length-scale parameters have crucial role on the nonlinear vibration of the structures[13] Belkhodja et al., investigated both thermal buckling and bending behavior of sandwich plates that have functionally graded (FGM) face layers. Their analysis employed a novel unified theoretical framework incorporating new quasi-three-dimensional and two-dimensional higher-order shear deformation theories (HSDTs). This framework accounts for both shear strain, captured by a newly introduced shape function, and the stretching effect[14]. Chu et al.[15]investigated the energy dissipation and the induced as well as intrinsic resonances of non-rectangular composite nanoplates with an undulating edge, supported by a medium exhibiting fractional torsional viscoelasticity. The nanostructure comprises a core of alumina fortified with graphene platelets (GPLs), enveloped by flexoelectric and magnetostrictive

materials as the superior and inferior layers, respectively. The assessment of dimensional influences is extrapolated from a novel theoretical perspective on local/nonlocal interactions within a biphasic framework used shear deformable ring theory Moosavi, H. et al studied the free in-plane vibration of nanoring based on elasticity theory Sahoo et al., focused on the geometrically nonlinear thermal frequencies of functionally graded (FG) sandwich structures. They employed numerical methods to analyze these frequencies, considering both linear and nonlinear variations in temperature distribution. To perform this numerical analysis, the researchers developed their own finite element code within MATLAB. This code incorporates advanced techniques such as higher-order shear deformation theory (HSDT) and Green-Lagrange nonlinear strain kinematics[16]. Khayat et al., examined a cylindrical shell with a special three-layered sandwich functionally graded material (S-FGM). This shell comprised an outer layer made of ceramic with the thickness, a middle layer (FGM) with the thickness, and an inner layer made of metal with the thickness. the initial temperature of the entire shell was assumed to be the same as the surrounding environment (ambient temperature). However, the outer layer was then subjected to a sudden and significant temperature change, known as a thermal shock[17]. Natarajan et Manickam studied the static and dynamic behavior of the sandwich plate FG using an 8-node quadrilateral plate element[18].Chu et al. [19]studied a theoretical assessment of the influence of a moving load and the integration of a piezoelectric patch on energy harvesting efficiency and the dynamic response of a Nano Conical Panel (NCP) composed of Shape Memory Alloy (SMA) situated atop a frictional foundation, utilizing the First-order Shear Deformation Theory (FSDT). Employing the mixture rule, the piezoelectric patch was enhanced with boron nitride nanotubes (BNNTs) known for their intelligent properties. To incorporate the effects at the nano-scale, a dual-phase nonlocal approach was implemented Mohammadi, M. et al extended a nonlocal elasticity theory to analyze the effect of the thermal environment on the vibration frequencies of mono-layer graphene sheet resting on elastic medium, it has been founded that the non-dimensional frequencies decreases with the increase of the temperature Akavci developed a new form of hyperbolic deformation function for the analysis of the different behaviors of the FG sandwich plate resting on the elastic Winkler-Pasternak foundation[20]. Using the FE formulation layer by layer based on the FSDT hypothesis (assumption), Pandey et Pradyumna examined the free vibration of the FG sandwich plate.[21]. Mohammadi et al. explored the impact of Coriolis effects on the vibrational behavior of a multilayer rotating piezoelectric nanobeam. The governing equations are derived based on nonlocal continuum and surface elasticity theories. Both axial and transverse governing equations are affected by the Coriolis effects. To determine the vibration frequencies of the multilayer piezoelectric nanobeams, we employ the differential quadrature method (DQM).Wan et al.[22]investigated the supersonic flutter characteristics and dependability of intelligent hybrid nanocomposite trapezoidal plates, taking into account a multitude of operational considerations. The structure undergoes analysis under yawed flow conditions, which is a common occurrence in supersonic aviation. Given the critical role that hybrid nanocomposites play in a range of fields, including aerospace and public safety devices, the study integrates a hybrid nanocomposite core layer fortified with carbon nanotubes (CNTs) and carbon fibers. This enhancement reflects the material's real-life complexities, such as fiber agglomeration, waviness, and stochastic fiber orientation, within the analytical framework. Mohammadi et al.examines how vibrations travel through layered, tiny beams made of a material that can convert pressure into electricity (piezoelectric). The researchers used a theory established for thicker beams (Timoshenko beam theory) to describe the equations that govern the movement of these rotating, ultra-thin beams. They then considered two advanced theories (nonlocal continuum theory and surface elasticity theory) to create a more precise equation that describes how these beams move. Mohammadi et al. examines how vibrations travel through tiny, layered beams made of a material that can convert pressure into electricity (piezoelectric). This research analysed these vibrations using established theories for thicker beams (Timoshenko beam theory) and considered more advanced theories (nonlocal continuum theory and surface elasticity theory) to create a more precise description of how these ultra-thin, spinning beams vibrate. Mohammadi et al. explores how a single layer of graphene (a single-layered graphene sheet, or SLGS) vibrates naturally when stretched (in-plane pre-load). The study considered two theories: one commonly used for thin plates (Kirchhoff plate theory) and another that accounts for the unique behavior of materials at very small scales (nonlocal elasticity theory). By combining these theories, a precise equation describing the vibration of the graphene sheet was derived. This equation predicts the vibration frequencies, with a special property of the material (the nonlocal parameter) affecting the calculations.

The main limitation of the present model compared to computational methods is the stretching effect. In other words, the present model could be only used for 2D plate theories. Moreover, the current theory uses four terms in kinematics and involves fewer governing equations than the conventional theories. Its solutions compare well with quasi-3D and 2D solutions. Additionally, this model simplifies the problem and considers the effect of transverse shear, which is not considered in the case of first and classical plate theories.

The aim of this work is to propose a theory with four unknowns to examine the hygrothermal-mechanical stability of a simply supported sandwich plate FG resting on a variable elastic foundation. The transverse shear effect is considered without any correction coefficient. The stability equations of the FG sandwich plate are derived

using the principle of virtual work, the Navier solution is retained for the resolution of this system of equation and for obtaining the critical buckling load. In addition, the effectiveness and accuracy of the current theory is confirmed by comparing the calculated results with those published. Then, several parametric studies are presented and discussed in details.

2. Mathematical formulation

The geometry and dimensions of the sandwich FG plate made are represented in Fig. 1. rectangular plate in FGM material of thickness "h", length "a" and width "b", are employed to describe infinitesimal deformations of a three-layer sandwich elastic plate

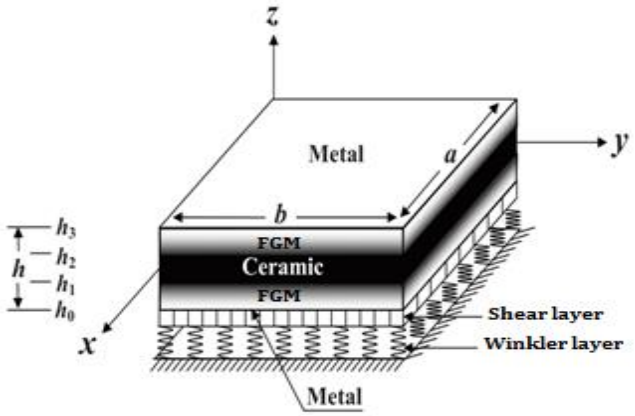

Fig 1: Geometries of the FGM plate

The material properties of each layer, such as thermal conductivity "K", Young's module "E", Poisson's ratio "ν", coefficient of thermal expansion "α" and coefficient of moisture expansion "β ", are influenced by various factors such as porosity. In this work, the effect of porosity is studied. Many porosity distribution models have been proposed by researchers to calculate the mechanical properties of materials of porous plates in FGM [23-26]. The porosities are distributed independently in each layer of the FGM sandwich plate. Four porosity models are used:

Uniform distribution of pores (Imperfect I):

$$\begin{cases} E^{(1)}(z) = (Ec - Em) * V^{(1)}(z) + Em - \dfrac{\zeta}{2}(Ec + Em) \\ E^{(3)}(z) = (Ec - Em) * V^{(3)}(z) + Em - \dfrac{\zeta}{2}(Ec + Em) \end{cases} \tag{1}$$

Non-uniform distribution of pores (Imperfect II):

$$\begin{cases} E^{(1)}(z) = (Ec - Em) * V^{(1)}(z) + Em - \dfrac{\zeta}{2}(Ec + Em)\left[1 - \dfrac{\left|2z - (h_0 + h_1)\right|}{h_1 - h_0}\right] \\ E^{(3)}(z) = (Ec - Em) * V^{(3)}(z) + Em - \dfrac{\zeta}{2}(Ec + Em)\left[1 - \dfrac{\left|2z - (h_3 + h_2)\right|}{h_3 - h_2}\right] \end{cases} \tag{2}$$

Non-uniform logarithmic distribution of pores (Imperfect III):

$$\begin{cases} E^{(1)}(z) = (Ec - Em) * V^{(1)}(z) + Em - \log\left(1 + \dfrac{\zeta}{2}\right)(Ec - Em)\left[1 - \dfrac{\left|2z - \left(h_0 + h_1\right)\right|}{h_1 - h_0}\right] \\ E^{(3)}(z) = (Ec - Em) * V^{(3)}(z) + Em - \log\left(1 + \dfrac{\zeta}{2}\right)(Ec - Em)\left[1 - \dfrac{\left|2z - \left(h_3 + h_2\right)\right|}{h_3 - h_2}\right] \end{cases} \tag{3}$$

Non-uniform linear distribution of pores (Imperfect IV):

$$\begin{cases} E^{(1)}(z) = (Ec - Em) * V^{(1)}(z) + Em + \dfrac{\zeta}{2}(Ec + Em)\left[1 - \dfrac{z - h_1}{h_0 - h_1}\right] \\ E^{(3)}(z) = (Ec - Em) * V^{(3)}(z) + Em + \dfrac{\zeta}{2}(Ec + Em)\left[1 - \dfrac{z - h_1}{h_0 - h_1}\right] \end{cases} \tag{4}$$

with "V$^{((j))}$ is the volume fraction of the layer « j » given by:

$$\begin{aligned} V1(z) &= \left(\frac{z - h_0}{h_1 - h_0}\right)^k, \quad && \lambda_1 = 1, \ \ z \in \left[h_0 ... h_1\right] \\ V2(z) &= 1 && \lambda_2 = 0, \ z \in \left[h_1 ... h_2\right] \\ V3(z) &= \left(\frac{z - h_3}{h_2 - h_3}\right)^k, \quad && \lambda_3 = 1, \ \ z \in \left[h_2 ... h_3\right] \end{aligned} \tag{5}$$

The plate is assumed to be resting on a two-parameter elastic foundation model that consists of closely spaced springs interconnected through a shear layer made up of incompressible vertical elements, which only deforms by transverse shear. The response equation "Rf" of this foundation is given by:

$$\delta U_f = \int_A f_e \delta w . dA = K_w w_0 - Kp\nabla^2 w_0$$

with "K¯" and "G¯" are the Winkler and Pasternak coefficients respectively, whose Winkler coefficient depends on x, is assumed to be linear, parabolic and sinusoidal [27-29](Sobhy 2015, Attia et al. 2018, Pradhan and Murmu 2009):

$$\overline{K}(x) = \frac{k_w h^3}{a^4}\left\{1 + \zeta\frac{x}{a} \quad 1 + \zeta(\frac{x}{a})^2 \quad 1 + \zeta\sin(\pi\frac{x}{a})\right\} \tag{6}$$

The displacement field of the theory proposes perhaps written according to[30-33]:

$$\begin{aligned} u(x, y, z) &= u_0(x, y) - z\frac{\partial w_0}{\partial x} + k_1 f(z)\int \theta dx \\ v(x, y, z) &= v_0(x, y) - z\frac{\partial w_0}{\partial y} + k_2 f(z)\int \theta dy \\ w(x, y, z) &= w_0(x, y) \end{aligned} \tag{7}$$

With $u_0(x, y)$, $v_0(x, y)$, $w_0(x, y)$, and $\theta(x, y)$ are the four unknowns of displacement of surface mean (average) of the plate.

Himeur et al [34] give the warping function retained:

$$f(z)=\sin\left(\frac{z}{h}-\frac{4z^3}{3h^2}\right) \tag{8}$$

The components of the deformation tensor are given by::

$$\begin{aligned}
&\varepsilon_{xx}=\varepsilon_{xx}^0+z\varepsilon_{xx}^1+f(z)\varepsilon_{xx}^2\\
&\varepsilon_{yy}=\varepsilon_{yy}^0+z\varepsilon_{yy}^1+f(z)\varepsilon_{yy}^2\\
&\gamma_{xy}=\gamma_{xy}^0+z\gamma_{xy}^1+f(z)\gamma_{xy}^2\\
&\gamma_{yz}=g(z)\gamma_{yz}^0\\
&\gamma_{xz}=g(z)\gamma_{xz}^0,\ g(z)=df(z)/dz
\end{aligned} \tag{9}$$

Where:

$$\begin{Bmatrix}\varepsilon_{xx}^0\\ \varepsilon_{yy}^0\\ \gamma_{xy}^0\end{Bmatrix}=\begin{Bmatrix}\dfrac{\partial u_0}{\partial x}\\ \dfrac{\partial v_0}{\partial y}\\ \dfrac{\partial u_0}{\partial y}+\dfrac{\partial v_0}{\partial x}\end{Bmatrix},\quad \begin{Bmatrix}\varepsilon_{xx}^1\\ \varepsilon_{yy}^1\\ \varepsilon_{xy}^1\end{Bmatrix}=\begin{Bmatrix}-\dfrac{\partial^2 w_0}{\partial x^2}\\ -\dfrac{\partial^2 w_0}{\partial y^2}\\ -2\dfrac{\partial^2 w_0}{\partial x\partial y}\end{Bmatrix} \tag{10a}$$

$$\begin{Bmatrix}\varepsilon_{xx}^2\\ \varepsilon_{yy}^2\\ \varepsilon_{xy}^2\end{Bmatrix}=\begin{Bmatrix}k_1A\dfrac{\partial^2\theta}{\partial x^2}\\ k_2B\dfrac{\partial^2\theta}{\partial y^2}\\ (k_1A+k_2B)\dfrac{\partial^2\theta}{\partial x\partial y}\end{Bmatrix},\quad \begin{Bmatrix}\gamma_{xz}^0\\ \gamma_{yz}^0\end{Bmatrix}=\begin{Bmatrix}k_1A\dfrac{\partial\theta}{\partial x}+\dfrac{\partial\varphi_z}{\partial x}\\ k_2B\dfrac{\partial\theta}{\partial y}+\dfrac{\partial\varphi_z}{\partial y}\end{Bmatrix} \tag{10b}$$

The Navier's method is used to solve the integral terms given in the displacement field and can be expressed as:

$$\int\theta dx=A\frac{\partial\theta}{\partial x},\quad \int\theta dy=B\frac{\partial\theta}{\partial y} \tag{11.a}$$

The coefficients k1, k2, A and B are given by:

$$k_1=\lambda^2,\qquad k_2=\mu^2,\quad A=-\frac{1}{\lambda^2},\quad B=-\frac{1}{\mu^2} \tag{11.b}$$

α and β are given by the expression (27).

2.1. The constitutive relations:

The constitutive relations of this plate can be expressed by:

$$\begin{Bmatrix}\sigma_{xx}\\ \sigma_{yy}\\ \tau_{xz}\\ \tau_{yz}\\ \tau_{xy}\end{Bmatrix}^{(n)} = \begin{bmatrix} C_{11} & C_{12} & 0 & 0 & 0\\ C_{12} & C_{11} & 0 & 0 & 0\\ 0 & 0 & C_{44} & 0 & 0\\ 0 & 0 & 0 & C_{55} & 0\\ 0 & 0 & 0 & 0 & C_{66}\end{bmatrix}^{(n)} \begin{Bmatrix}\varepsilon_{xx}-\alpha\Delta T\\ \varepsilon_{yy}-\alpha\Delta T\\ \gamma_{xz}\\ \gamma_{yz}\\ \gamma_{xy}\end{Bmatrix}^{(n)} \tag{12}$$

With

$$C_{11}^{(n)} = C_{22}^{(n)} = \frac{E^{(n)}(z)}{1-(\nu^{(n)})^2},\ C_{12}^{(n)} = \nu^{(n)} C_{11}^{(n)},\ C_{44}^{(n)} = C_{55}^{(n)} = C_{66}^{(n)} = \frac{E^{(n)}(z)}{2(1+\nu^{(n)})} \tag{13}$$

2.2. Stability equations:

The principle of virtual work for the FG sandwich plate under a hygrothermal-mechanical load can be expressed as[30, 35] :

$$\begin{aligned}&\iint [N_x\delta\varepsilon_x^0 + N_y\delta\varepsilon_y^0 + N_{xy}\delta\gamma_{xy}^0 + M_x^b\delta k_x^b + M_y^b\delta k_y^b + M_{xy}^b\delta k_{xy}^b + M_x^s\delta k_x^s + M_y^s\delta k_y^s + M_{xy}^s\delta k_{xy}^s\\ &+\left(S_{yz}^s\right)\delta\gamma_{yz}^0 + \left(S_{xz}^s\right)\delta\gamma_{xz}^0 - \left(\frac{N_x}{b}\frac{\partial^2 w}{\partial x^2} + \frac{N_y}{a}\frac{\partial^2 w}{\partial y^2} - R_f(w)\right)\delta w)]dxdy = 0\end{aligned} \tag{14}$$

The resulting forces and moments are defined by:

$$\begin{Bmatrix} N_x & N_y & N_{xy}\\ M_x^b & M_y^b & M_{xy}^b\\ M_x^s & M_y^s & M_{xy}^s\end{Bmatrix} = \sum_{j=1}^{3}\int_{h_{j-1}}^{h_j}\left(\sigma_x,\sigma_y,\tau_{xy}\right)\begin{Bmatrix}1\\ z\\ f(z)\end{Bmatrix}dz \tag{15.a}$$

And

$$\left(S_{xz}^s, S_{yz}^s\right) = \sum_{j=1}^{3}\int_{h_{j-1}}^{h_j}\left(\tau_{xz},\tau_{yz}\right) g(z)\, dz \tag{15.b}$$

Replacing the Eq. (10) in Eq. (12) and the result in the equation. (15) The resultants of the forces and moments are obtained in matrix form as:

$$\begin{Bmatrix} N\\ M^b\\ M^s\end{Bmatrix} = \begin{bmatrix} A & B & B^s\\ B & D & D^s\\ B^s & D^s & H^s\end{bmatrix}\begin{Bmatrix}\varepsilon\\ k^b\\ k^s\end{Bmatrix} - \begin{Bmatrix} N^T\\ M^{bT}\\ M^{sT}\end{Bmatrix} - \begin{Bmatrix} N^C\\ M^{bC}\\ M^{sC}\end{Bmatrix},\ S = A^s\gamma \tag{16.a}$$

$$\begin{aligned} N &= \left\{N_x, N_y, N_{xy}\right\}^t, M^b = \left\{M_x^b, M_y^b, M_{xy}^b\right\}^t\\ M^s &= \left\{M_x^s, M_y^s, M_{xy}^s\right\}^t\end{aligned} \tag{16.b}$$

$$N^T=\left\{N_x^T,N_y^T,0\right\}^t,M^{bT}=\left\{M_x^{bT},M_y^{bT},0\right\}^t$$
$$M^{sT}=\left\{M_x^{sT},M_y^{sT},0\right\}^t \tag{16.c}$$

$$N^C=\left\{N_x^C,N_y^C,0\right\}^t,M^{bC}=\left\{M_x^{bC},M_y^{bC},0\right\}^t$$
$$M^{sC}=\left\{M_x^{sC},M_y^{sC},0\right\}^t \tag{16.d}$$

With A_{11}, B_{11} etc are rigidity components given by:

$$\begin{Bmatrix} A_{11} & B_{11} & D_{11} & B_{11}^s & D_{11}^s & H_{11}^s \\ A_{12} & B_{12} & D_{12} & B_{12}^s & D_{12}^s & H_{12}^s \\ A_{66} & B_{66} & D_{66} & B_{66}^s & D_{66}^s & H_{66}^s \end{Bmatrix}=\sum_{j=1}^{3}\int_{h_{j-1}}^{h_j} C_{11}\left(1,z,z^2,f(z),zf(z),f^2(z)\right)\begin{Bmatrix} 1 \\ \nu \\ \dfrac{1-\nu}{2} \end{Bmatrix}dz \tag{16.e}$$

$$\left(A_{22},B_{22},D_{22},B_{22}^s,D_{22}^s,H_{22}^s\right)=\left(A_{11},B_{11},D_{11},B_{11}^s,D_{11}^s,H_{11}^s\right)$$

$$A_{44}^s=A_{55}^s=\sum_{j=1}^{3}\int_{h_{j-1}}^{h_j} C_{44}^{(j)}\left[g(z)\right]^2dz,$$

The resultants of the forces and moments due to hygrothermal loading are given by:

$$\begin{Bmatrix} N_x^{\Theta} \\ M_x^{b\Theta} \\ M_x^{s\Theta} \end{Bmatrix}=\sum_{j=1}^{3}\int_{h_{j-1}}^{h_j}\frac{E^{(j)}(z)}{1-\nu}\Upsilon^{(j)}(z)\Theta(z)\begin{Bmatrix} 1 \\ z \\ f(z) \end{Bmatrix}dz \tag{17}$$

With

$$\Theta(z)=\begin{cases} C(z) & \text{if } \Upsilon=\beta \\ T(z) & \text{if } \Upsilon=\alpha \end{cases} \tag{18}$$

Assuming the terms of displacementsu_0^0; v_0^0; w_0^0 and θ^0 of the equilibrium state of the FG sandwich plate under hygrothermal loading. Using the termsu_0^1; v_0^1; w_0^1 et θ^1 which represent the adjacent equilibrium state. General trips correspond to [30, 36] are:

$$u_0=u_0^0+u_0^1,\ v_0=v_0^0+v_0^1,\ w_0=w_0^0+w_0^1,\ \theta_0=\theta_0^0+\theta_0^1 \tag{19}$$

The stability equations of the plate can be obtained by the adjacent equilibrium criterion such as:

$$\frac{\partial N_x^1}{\partial x}+\frac{\partial N_{xy}^1}{\partial y}=0$$

$$\frac{\partial N_{xy}^1}{\partial x}+\frac{\partial N_y^1}{\partial yx}=0$$

$$-\frac{\partial^2 M_x^{b1}}{\partial x^2}-2\frac{\partial^2 M_{xy}^{b1}}{\partial x\partial y}-\frac{\partial^2 M_y^{b1}}{\partial y^2}-\overline{N}+R_f=0 \tag{20}$$

$$-\left(M_x^{s1}k_1+M_y^{s1}k_2\right)+\frac{\partial S_{xz}^{s1}}{\partial x}k_1A'+\frac{\partial S_{yz}^{s1}}{\partial y}k_2B'$$

$$-\left(k_1A'+k_2B'\right)\frac{\partial M_{xy}^{s1}}{\partial x\partial y}=0$$

With

$$\overline{N}\ =N_x^0\frac{\partial^2\left(w_0^1\right)}{\partial x^2}+N_y^0\frac{\partial^2\left(w_0^1\right)}{\partial y^2}+N_{xy}^0,\quad N_{xy}^0=0 \tag{21}$$

In which N_x^0 et N_y^0 are:

$$N_x^0=N_x^M+N_x^H,\ N_y^0=N_y^M+N_y^M$$

$$N_x^M=-\frac{N_x}{b},\ N_y^M=-\frac{N_y}{a},\ \frac{N_x^M}{N_y^M}=R \tag{22.a}$$

$$N_x^H=N_y^H=-\sum_{j=1}^{3}\int_{h_{j-1}}^{h_j}\frac{E^{(j)}(z)}{1-\nu}\left(\alpha^{(j)}(z)T(z)+\beta^{(j)}(z)C(z)\right)dz \tag{22.b}$$

2.3. Variation of the hygrothermal load:

In this study, the FG plate is subjected to three types of hygrothermal distributions through the thickness (Uniform, linear and non-linear). Each type of hygrothermal distribution is described in detail in the following:

2.3.1. Uniform variation (UVT)

In the first type, the FG sandwich plate is subjected to an initial temperature and humidity and, then the humidity and temperature were uniformly increased to the final values With

$$\Delta\Theta=\Theta_f-\Theta_i,\ \ \Theta=\mathrm{T,\ C} \tag{23}$$

2.3.2. Linear variation (LVT)

The second type of hygrothermal distribution is linear and can be presented in the following form:

$$\Theta\left(z\right)=\Theta_l+\Delta\Theta\left(\frac{1}{2}+\frac{z}{h}\right)$$

$$\Delta\Theta=\Theta_u-\Theta_l,\ \ \Theta=\mathrm{T,\ C} \tag{24}$$

With Θ_u and Θ_l are the temperature and humidity values at the bottom and top surface of the FG sandwich plate and $\Delta\Theta=\Theta_u-\Theta_l$.

2.3.3. Non-linear variation (NLVT)

In this case, the temperature of the upper surface is Tt and it is considered that it varies from Tt to Tb in which the plate is deformed, according to the variation of the power law through the thickness, up to the temperature of lower surface Tb. As a result, the increase of the temperature through the thickness is given by:

$$\Theta(z) = \Theta_l + \Delta\Theta\left(\frac{1}{2} + \frac{z}{h}\right)^{\gamma} \tag{25}$$

where is the hygrothermal exponent $1\langle\gamma\langle\infty$.

2.4. Analytical solution

Based on the Navier's solution[30, 37, 38], the displacement components which satisfy the boundary conditions are given by:

$$\begin{Bmatrix} u_0^1 \\ v_0^1 \\ w_0^1 \\ \theta^1 \end{Bmatrix} = \sum_{m=1}^{\infty}\sum_{n=1}^{\infty} \begin{Bmatrix} U_{mn}\cos(\lambda x)\sin(\mu y) \\ V_{mn}\sin(\lambda x)\cos(\mu y) \\ W_{mn}\sin(\lambda x)\sin(\mu y) \\ \mathrm{X}_{mn}\sin(\lambda x)\sin(\mu y) \end{Bmatrix} \tag{26}$$

With U_{mn}, V_{mn}, W_{mn}, X_{mn} are arbitrary parameters to be determined. μ and β are defined by:

$$\lambda = \frac{m\pi}{a} \text{ and } \mu = \frac{n\pi}{b} \tag{27}$$

Replacing the Eq. (26) in Eq. (19), the critical buckling load solution of the FGM sandwich plate can be obtained:

$$\begin{bmatrix} a_{11} & a_{12} & a_{13} & a_{14} \\ a_{21} & a_{22} & a_{23} & a_{24} \\ a_{31} & a_{32} & a_{33} & a_{34} \\ a_{41} & a_{42} & a_{43} & a_{44} \end{bmatrix} \begin{Bmatrix} U_{mn} \\ V_{mn} \\ W_{mn} \\ \mathrm{X}_{mn} \end{Bmatrix} = \begin{Bmatrix} 0 \\ 0 \\ 0 \\ 0 \end{Bmatrix} \tag{28}$$

With

$$\begin{aligned}
&a_{11} = -(A_{11}\lambda^2 + A_{66}\mu^2),\ a_{12} = -\lambda\mu(A_{12} + A_{66}),\ a_{13} = \lambda(B_{11}\lambda^2 + (B_{12} + 2B_{66})\mu^2) \\
&a_{14} = -\lambda(B_{11}{}^s A'k_1\lambda^2 + B_{12}{}^s B'k_2\mu^2 + B_{66}{}^s(A'k_1 + B'k_2)\mu^2) \\
&a_{22} = -\lambda^2 A_{66} - \mu^2 A_{22},\ a_{23} = \mu(B_{22}\mu^2 + (B_{12} + 2B_{66})\lambda^2) \\
&a_{24} = -\mu(B_{22}{}^s A'k_1\mu^2 + B_{12}{}^s B'k_2\lambda^2 + B_{66}{}^s(A'k_1 + B'k_2)\lambda^2) \\
&a_{33} = -\lambda^2(D_{11}\lambda^2 + (2D_{12} + 4D_{66})\mu^2) - D_{22}\mu^4 + N_x^0\lambda^2 + N_y^0\mu^2 - K_w - K_p(\lambda^2 + \mu^2) \\
&a_{34} = D_{11}{}^s A'k_1\lambda^4 + D_{12}{}^s(A'k_1 + B'k_2)\lambda^2\mu^2 + D_{22}{}^s B'k_2\mu^4 + 2D_{66}{}^s(A'k_1 + B'k_2)\lambda^2\mu^2 \\
&a_{44} = -(H_{11}{}^s\lambda^2 k_1 + 2k_1\mu^2 H_{66}{}^s + 2H_{66}{}^s\lambda^2 k_2 + H_{12}{}^s\lambda^2 k_2 + k_1\mu^2 H_{12}{}^s + k_2\mu^2 H_{22}{}^s \\
&\qquad + A_s^{44}k_1 + A_s^{55}k_2)
\end{aligned} \tag{29}$$

To obtain the non-trivial solution, the determinant $|A|$ should be zero. By solving the equation $|A|=0$, one can easily obtain the critical buckling load $\bar{N}=P_x$ and the critical buckling temperature $\bar{N}=\Delta T_{cr}$, $P_x=P_y=0$.

3. Results and discussion

3.1. Comparative analysis:

To verify the validity of the presented model, an FGM sandwich plate is used to compare the model's results with those of Menasria et al[31] and Bourada et al[39]. Therefore, two different materials are used. These are the alloy of titanium (Ti-6A1-4V) -Zirconia (ZrO2) and aluminum (Al) -Alumina (Al2O3). Tables 2, 3 and 4, represent results obtained for different types of sandwich plates of graded evaluated materials subjected to a uniform thermal load, linear and non-linear through the thickness compared with other theories of plates. The critical temperature variation (Tcr = 10-3ΔTcr) is determined for k = 0, 1, 2, 5 and ∞ and for different types of temperature distribution, as shown in the tables. We can see in the three tables that there is a very good correlation between the used theory and the other theories. The properties used in Tables 2,3 and 4 are:

Ec=244.27 GPa, αc=12.766x10^(-6)/°C, E_m=66.2 GPa, α_m=10.3x10^(-6)/°C. While the properties used in table 5 are:

E_c=380 GPa, α_c=7.4x10^(-6)/°C, E_m=70 GPa and for table 6 and 7: E_c=151 GPa, α_c=7.4x10^(-6)/°C, E_m=70 GPa, with a constant Poisson's ratio« υ=0.3 ». The properties retained for the analysis of hygrothermal behavior are given in the following table:

Table 1: Material properties of the plate

Material	Silicon nitride (Si_3N_4)	stainless steel (SUS304)
E	348.43	201.04
α	5.8711	12.330
K	13.723	15.379
β	0.001	0.44
ν	0.3	

All the results presented in this work are calculated using the following dimensionless parameter:

$$\bar{N}_{cr}=\frac{N_{cr}a^2}{E_m h^3}$$

Table 2: The critical buckling temperature T_{cr} of a square sandwich plate under a uniform temperature variation (a/h= 5).

k	Theory	(1-0-1)	(1-1-1)	(2-1-2)	(3-1-3)
0	**Present**	**3,23742**	**3,23742**	**3,23742**	**3,23742**
	Menasria et al [31]	3,24034	3,24034	3,24034	3,24034
	Bourada et al[39]	3.23652	3.23652	3.23652	3.23652
1	**Present**	**2,68530**	**2,58812**	**2,59065**	**2,60646**
	Menasria et al [31]	2,69376	2,59191	2,59707	2,61374
	Bourada et al[39]	2.68781	2.58882	2.59241	2.60856
2	**Present**	**2,62551**	**2,35816**	**2,39307**	**2,43596**
	Menasria et al[31]	2,63896	2,36407	2,39953	2,44692
	Bourada et al [39]	2.63018	2.36000	2.39637	2.43977
5	**Present**	**2,92612**	**2,20652**	**2,34322**	**2,45653**
	Menasria et al[31]	2,94934	2,21632	2,35871	2,47451
	Bourada et al [39]	2.93446	2.21009	2.34898	2.46321
∞	**Present**	**4,01251**	**4,01251**	**4,01251**	**4,01251**
	Menasria et al[31]	4,01613	4,01613	4,01613	4,01613
	Bourada et al[39]	4.01293	4.01293	4.01293	4.01293

Table 1: The critical buckling temperature T_{cr} of a square sandwich plate under a linear temperature variation (γ=1 et a/h= 5).

k	Theory	(1-0-1)	(1-1-1)	(2-1-2)	(3-1-3)
0	**Present**	**6,42484**	**6,42484**	**6,42484**	**6,42484**
	Menasria et al [31]	6,43068	6,43068	6,43068	6,43068
	Bourada et al [39]	6.42305	6.42305	6.42305	6.42305

1	**Present**	**5,32061**	**5,12624**	**5,13129**	**5,16293**
	Menasria et al [31]	5,33752	5,13382	5,14414	5,17747
	Bourada et al [39]	5.32562	5.12765	5.13482	5.16711
2	**Present**	**5,20102**	**4,66632**	**4,73615**	**4,82191**
	Menasria et al [31]	5,22793	4,67814	4,75538	4,84385
	Bourada et al [39]	5.21036	4.66999	4.74275	4.82954
5	**Present**	**5,80224**	**4,36303**	**4,63645**	**4,86305**
	Menasria et al [31]	5,84868	4,38263	4,66742	4,89903
	Bourada et al [39]	5.81891	4.37017	4.64797	4.87641
∞	**Present**	**7,97503**	**7,97503**	**7,97503**	**7,97503**
	Menasria et al [31]	7,98226	7,98226	7,98226	7,98226
	Bourada et al [39]	7.97281	7.97281	7.97281	7.97281

Table 4: The critical buckling temperature Tcr of a square sandwich plate under a non-linear temperature variation (γ=5 et a/h= 5).

k	Theory	(1-0-1)	(1-1-1)	(2-1-2)	(3-1-3)
0	**Present**	**19,27450**	**19,27450**	**19,27450**	**19,27450**
	Menasria et al [31]	19,29203	19,29203	19,29203	19,29203
	Bourada et al [39]	19.26915	19.26915	19.26915	19.26915
1	**Present**	**22,38960**	**21,68600**	**21,96770**	**22,08670**
	Menasria et al [31]	22,46081	21,71806	22,02269	22,12553
	Bourada et al [39]	22.41074	21.69196	21.98279	22,14890
2	**Present**	**22,98800**	**21,96570**	**22,32160**	**22,49500**
	Menasria et al [31]	23,10689	22,02137	22,41227	22,59731
	Bourada et al [39]	23.02926	21.98304	22.35275	22.53055
5	**Present**	**23,64170**	**22,02710**	**22,55880**	**22,84740**
	Menasria et al [31]	23,83092	22,12608	22,70953	23,01642
	Bourada et al [39]	23.70963	22.06317	22.61489	22.91015
∞	**Present**	**23,92510**	**23,92510**	**23,92510**	**23,92510**
	Menasria et al [31]	23,94679	23,94679	23,94679	23,94679
	Bourada et al [39]	23.91843	23.91843	23.91843	23.91843

The stability of FG plates (Al/Al2O3) under mechanical loading is studied by considering two types of loading in the plane: uniaxial compression (γ=0), bi-axial compressions (γ=1). The obtained results are presented in Table 5. It can be seen that the current results are again in good agreement with the results of Sekkal et al (2017), Nguyen (2015) and Thai and Choi (2012). The mechanical properties retained for the determination of the critical buckling load are shown in the following table:

Table 2: Dimensionless critical load Ncr of a rectangular plate made of functionally graded material (FGM) (γ= 0,1 et a/b=0.5).

γ	*a/h*	Theory	Material index ''*k*''				
			0	**0.5**	**1**	**5**	**10**
0	**5**	**Present**	**6,7217**	**4,4243**	**3,4170**	**2,1531**	**1,9240**
		Sekkal & al [40]	6.7005	4.4728	3.4983	2.2076	1.9459
		Thai & Choi [41]	6.7203	4.4235	3.4164	2.1484	1.9260
		Nguyen 2015	6.7417	4.4343	3.4257	2.1459	1.9213
	10	**Present**	**7,4059**	**4,8209**	**3,7113**	**2,4180**	**2,1906**
		Sekkal & al [40]	7.4126	4.8904	3.8221	2.5090	2.2374
		Thai & Choi [41]	7.4053	4.8206	3.7111	2.4165	2.1896
		Nguyen 2015	7.4115	4.8225	3.7137	2.4155	2.1911
	20	**Present**	**7,5994**	**4,9316**	**3,7931**	**2,4949**	**2,2693**
		Sekkal & al [40]	7.6109	5.0028	3.9108	2.5963	2.3230
		Thai & Choi [41]	7.5993	4.9315	3.7930	2.4944	2.2690
		Nguyen 2015	7.6009	4.9307	3.7937	2.4942	2.2695
1	**5**	**Present**	**5,3774**	**3,5394**	**2,7336**	**1,7224**	**1,5391**
		Sekkal & al [40]	5.3604	3.5783	2.7987	1.7661	1.5568
		Thai & Choi [41]	5.3762	3.5388	2.7331	1.7187	1.5370
		Nguyen 2015	5.3934	3.5475	2.7406	1.7167	1.5408
	10	**Present**	**5,9247**	**3,8567**	**2,9690**	**1,9344**	**1,7524**
		Sekkal & al [40]	5.9301	3.9123	3.0577	2.0072	1.7899
		Thai & Choi [41]	5.9243	3.8565	2.9689	1.9332	1.7517
		Nguyen 2015	5.9292	3.8580	2.9710	1.9324	1.7529
	20	**Present**	**6,0794**	**3,9453**	**3,0344**	**1,9959**	**1,8154**
		Sekkal & al [40]	6.0887	4.0022	3.1287	2.0770	1.8584
		Thai & Choi [41]	6.0794	3.9452	3.0344	1.9955	1.8152
		Nguyen 2015	6.0807	3.9445	3.0350	1.9953	1.8156

3.2. Parametric study

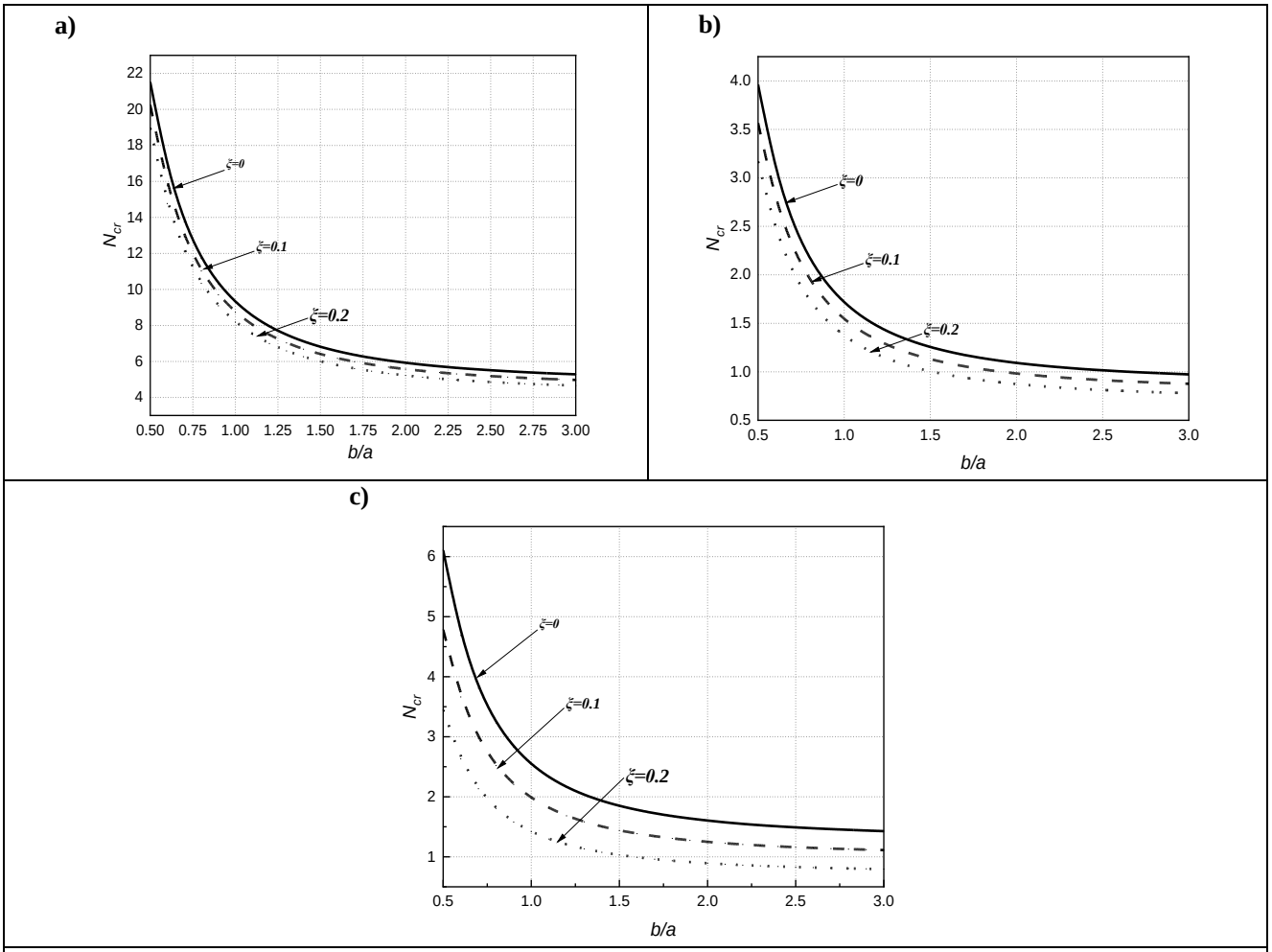

Fig 2: Evolution of the critical buckling load of a sandwich plate (1-0-1) with: a) k=0, b) k=∞, c) k=2, depending on the geometric ratio « b/a » for different values of « ξ » , (a/h=10).

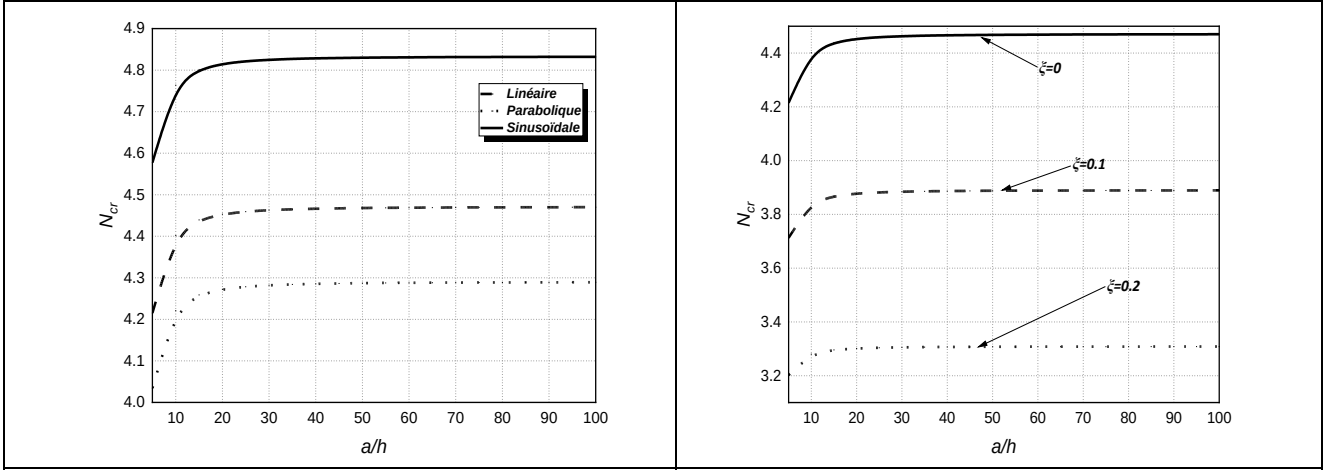

Fig 3: Variation of the critical buckling load of a square FG plate on a variable foundation (k=2, ξ=0, ζ=10, kw=kg=100).

Fig 4: Variation of the critical buckling load of a square FG plate on a linear foundation (k=2, ζ=10, kw=kg=100).

Figure 2. Shows the variation of the critical buckling load of three types of plates: ceramic, metallic and functionally graduated material (FGM) under mechanical loading and under the effect of porosity, and as shown in the figure, this critical buckling load decreased with increasing geometric ratio« b/a » and coefficient of porosity (ξ). For the two figures 3 and 4, the critical buckling load Ncr increases with the increase in the thickness ratio « a/h » to reach a maximum value for a ratio (a/h=10) and then stabilizes for the values (a/h>10), for curve 3 also represents

the variation of the critical buckling load depending on the type of foundation used and ,as shown in the figure, the obtained values for a sinusoidal foundation are greater than those for parabolic foundations , while linear foundations take intermediate values, when the porosity coefficient does not influence the shape of the curve but it decrease the critical buckling load because of its influence on stiffens of the plate .

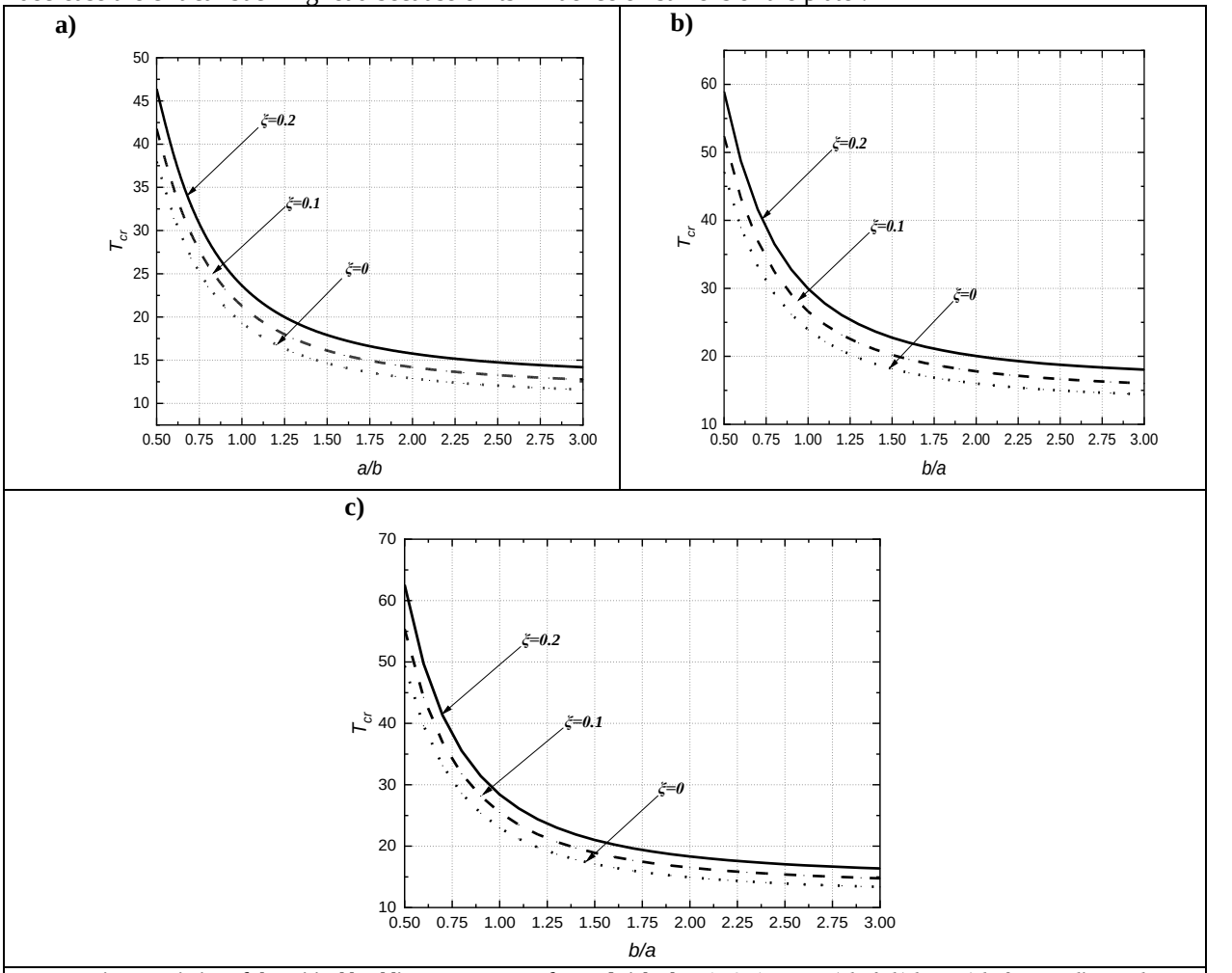

Fig 5: Variation of the critical buckling temperature of a sandwich plate (1-0-1) avec : a) k=0, b) k=∞, c) k=2, according to the geometrical ratio « b/a » for different values of « ξ » , (a/h=10).

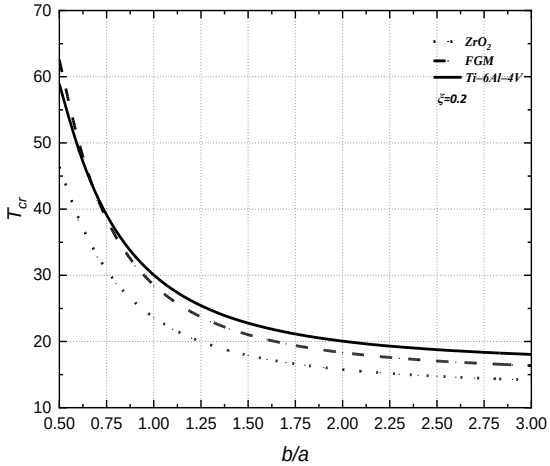

Fig 6: Comparison of the critical buckling temperature of a plate: fully ceramic, fully metallic and FG sandwich (1-0-1), depending on the geometric ratio « b/a » , (k=2 , ξ=0.2 a/h=10).

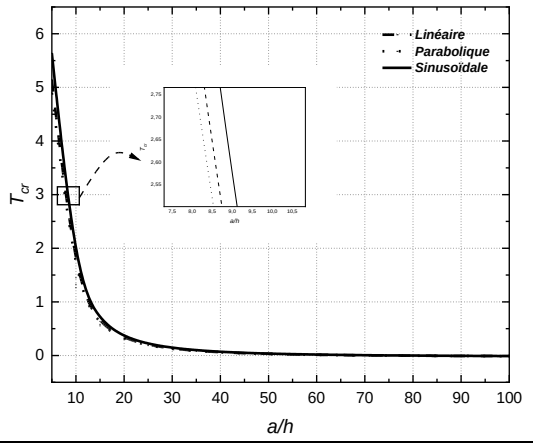

Fig 7: Variation of the critical buckling load of a square FG plate on a variable foundation (k=2, ξ=0, kw=kg=100).

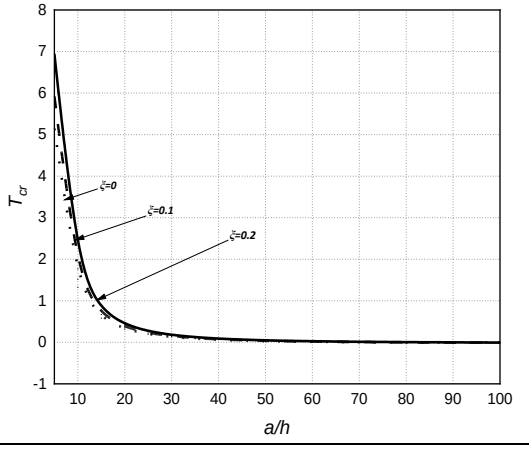

Fig 8: Variation of the critical buckling load of a square FG plate on a linear foundation (a=b, k=2, kw=kg=100).

Figure 5. Shows the change in critical buckling temperature for three types of plate: ceramic, metallic and functionally graduated (FGM) under the effect of porosity. It can be seen that the critical buckling decreasing with the increasing geometric "b / a" ratio such as the including of the porosity reduce the value of the critical buckling when the porosity coefficient increases and this because of its effect on the stiffness of the plate. Figure 6 shows a comparison between the three types of plate, whose values obtained for an FGM plate are between those of an all-ceramic and all-metal plate. Figure 7. Shows variation of Tcr of a plate resting on three types of elastic foundation as a function of the thickness ratio "a / h". The same study for figure 8, but with a linear foundation and different values of the coefficient of porosity. In both cases, the critical buckling temperature decreased with the increase in the "a / h" ratio with a slight deviation caused by the type of foundation used in Figure 7 and the value of the porosity coefficient for Figure 8.

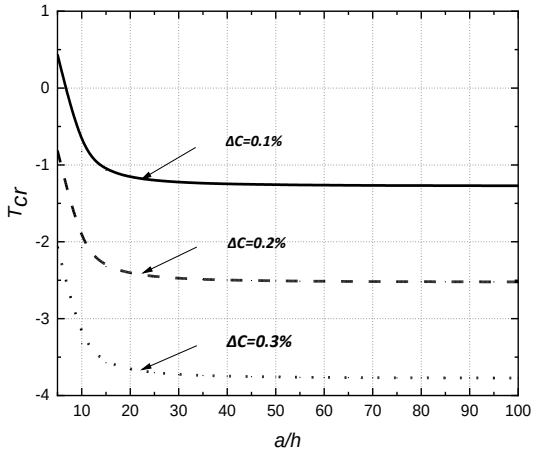

Fig 9: Change in the critical buckling temperature of an FG plate under the effect of humidity according on the aspect ratio « a/h », (a=b, k=2, kw=kg=0).

Figure 9. Shows the variation of Tcr according to the “a / h” ratio for different humidity values, for the three humidity proportions the critical buckling temperature decreases rapidly with the increase in the « a/h » ratio and takes its minimum value for (a/h=30), and the rest of the curve is purely lowered.

a) b)

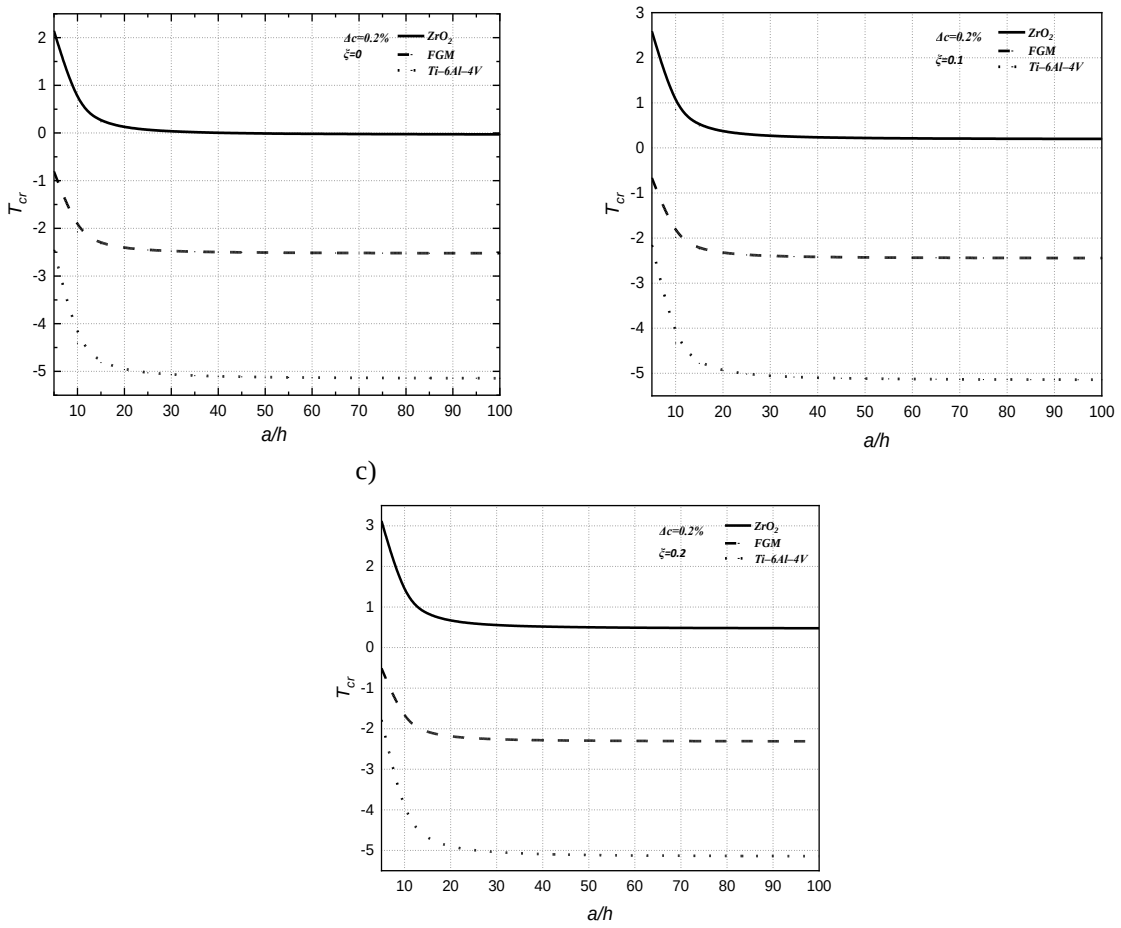

Fig 10: Variation of Tcr according to the ratio « a/h » of a plate: a) perfect « ξ=0 », b) porous « ξ=0.1 » and c) porous « ξ=0.2 », for (a=b, k=2, kw=kg=0)

Figure 10. Shows the variation of Tcr depending on the « a/h or three values of the porosity coefficient (for curve (a) « ξ=0 », (b) « ξ=0.1 » et (c) « ξ=0.2 ») with a humidity level ΔC=0,2. Thus the critical buckling temperature decreases rapidly with increasing "a/h" ratio and takes its minimum value for (a/h = 30), and the rest of the curve is purely lowered.

4. **Conclusions**

In the present work, the mechanical and hygrothermal stability of an FG sandwich plate resting on a variable elastic foundation is investigated, using a higher-order shear deformation theory including indeterminate integral terms. The plate stability equations are derived via the principle of virtual work. From the obtained results and the comparisons, we can conclude that:

- The current theory is precise and efficient for determining the critical buckling values of plates subjected to hygro-thermo-mechanical loads.
- Whatever the type of loading, the critical buckling value decreases with the increase in the geometric ratio "a/b" and increases with the increase in the thickness ratio "a/h".
- The lowest values of the critical buckling load are given for the porous plate in the case of mechanical load. However, the highest values of the critical buckling temperature are given for porous plates.
- Increasing the elastic foundation's parameters (K_w, K_p) decreases the critical buckling load.
- The rise in moisture concentration causes a rapid critical buckling temperature decrease.

Finally, an improvement of the current formulation will be considered in future works to account for the effect of thickness stretching using models of quasi-3D shear deformation theories.

References

[1] M. Gu, X. Cai, Q. Fu, H. Li, X. Wang, B. Mao, Numerical analysis of passive piles under surcharge load in extensively deep soft soil, *Buildings*, Vol. 12, No. 11, pp. 1988, 2022.

[2] X. Gong, L. Wang, Y. Mou, H. Wang, X. Wei, W. Zheng, L. Yin, Improved four-channel PBTDPA control strategy using force feedback bilateral teleoperation system, *International Journal of Control, Automation and Systems*, Vol. 20, No. 3, pp. 1002-1017, 2022.

[3] M. A. Al-Osta, Wave propagation investigation of a porous sandwich FG plate under hygrothermal environments via a new first-order shear deformation theory, *Steel and Composite Structures*, Vol. 43, No. 1, pp. 117, 2022.

[4] P. Wan, M. Al-Furjan, R. Kolahchi, L. Shan, Application of DQHFEM for free and forced vibration, energy absorption, and post-buckling analysis of a hybrid nanocomposite viscoelastic rhombic plate assuming CNTs' waviness and agglomeration, *Mechanical Systems and Signal Processing*, Vol. 189, pp. 110064, 2023.

[5] A. Hajlaoui, E. Chebbi, F. Dammak, Three-dimensional thermal buckling analysis of functionally graded material structures using a modified FSDT-based solid-shell element, *International Journal of Pressure Vessels and Piping*, Vol. 194, pp. 104547, 2021.

[6] M. Mohammadi, M. Safarabadi, A. Rastgoo, A. Farajpour, Hygro-mechanical vibration analysis of a rotating viscoelastic nanobeam embedded in a visco-Pasternak elastic medium and in a nonlinear thermal environment, *Acta Mechanica*, Vol. 227, pp. 2207-2232, 2016.

[7] J. Mantari, E. Granados, A refined FSDT for the static analysis of functionally graded sandwich plates, *Thin-Walled Structures*, Vol. 90, pp. 150-158, 2015.

[8] M. Sobhy, Buckling and free vibration of exponentially graded sandwich plates resting on elastic foundations under various boundary conditions, *Composite Structures*, Vol. 99, pp. 76-87, 2013.

[9] V.-H. Nguyen, T.-K. Nguyen, H.-T. Thai, T. P. Vo, A new inverse trigonometric shear deformation theory for isotropic and functionally graded sandwich plates, *Composites Part B: Engineering*, Vol. 66, pp. 233-246, 2014.

[10] M. Al-Furjan, S. Fan, L. Shan, A. Farrokhian, X. Shen, R. Kolahchi, Wave propagation analysis of micro air vehicle wings with honeycomb core covered by porous FGM and nanocomposite magnetostrictive layers, *Waves in Random and Complex Media*, pp. 1-30, 2023.

[11] L. Shan, C. Tan, X. Shen, S. Ramesh, M. Zarei, R. Kolahchi, M. Hajmohammad, The effects of nano-additives on the mechanical, impact, vibration, and buckling/post-buckling properties of composites: A review, *Journal of Materials Research and Technology*, 2023.

[12] M. Chitour, A. Bouhadra, F. Bourada, B. Mamen, A. A. Bousahla, A. Tounsi, A. Tounsi, M. A. Salem, K. M. Khedher, Stability analysis of imperfect FG sandwich plates containing metallic foam cores under various boundary conditions, in *Proceeding of*, Elsevier, pp. 106021.

[13] M. Mohammadi, M. Hosseini, M. Shishesaz, A. Hadi, A. Rastgoo, Primary and secondary resonance analysis of porous functionally graded nanobeam resting on a nonlinear foundation subjected to mechanical and electrical loads, *European Journal of Mechanics-A/Solids*, Vol. 77, pp. 103793, 2019.

[14] Y. Belkhodja, M. E. A. Belkhodja, H. Fekirini, D. Ouinas, New quasi-three-, and two-dimensional trigonometric-cubic monomial HSDT for thermal buckling and thermo-mechanical bending analyses of FGM symmetrical/non-symmetrical sandwich plates with hard/soft core, *Composite Structures*, Vol. 304, pp. 116402, 2023.

[15] C. Chu, L. Shan, M. Al-Furjan, A. Farrokhian, R. Kolahchi, Energy absorption, free and forced vibrations of flexoelectric nanocomposite magnetostrictive sandwich nanoplates with single sinusoidal edge on the frictional torsional viscoelastic medium, *Archives of Civil and Mechanical Engineering*, Vol. 23, No. 4, pp. 223, 2023.

[16] B. Sahoo, N. Sharma, B. Sahoo, P. M. Ramteke, S. K. Panda, S. Mahmoud, Nonlinear vibration analysis of FGM sandwich structure under thermal loadings, in *Proceeding of*, Elsevier, pp. 1392-1402.

[17] M. Khayat, A. Baghlani, M. A. Najafgholipour, A hybrid algorithm for modeling and studying of the effect of material and mechanical uncertainties on stability of sandwich FGM materials under thermal shock, *Composite Structures*, Vol. 293, pp. 115657, 2022.

[18] S. Natarajan, G. Manickam, Bending and vibration of functionally graded material sandwich plates using an accurate theory, *Finite Elements in Analysis and Design*, Vol. 57, pp. 32-42, 2012.

[19] C. Chu, M. Al-Furjan, R. Kolahchi, Energy harvesting and dynamic response of SMA nano conical panels with nanocomposite piezoelectric patch under moving load, *Engineering Structures*, Vol. 292, pp. 116538, 2023.

[20] S. Akavci, Mechanical behavior of functionally graded sandwich plates on elastic foundation, *Composites Part B: Engineering*, Vol. 96, pp. 136-152, 2016.

[21] S. Pandey, S. Pradyumna, Free vibration of functionally graded sandwich plates in thermal environment using a layerwise theory, *European Journal of Mechanics-A/Solids*, Vol. 51, pp. 55-66, 2015.

[22] P. Wan, M. Al-Furjan, R. Kolahchi, Nonlinear flutter response and reliability of supersonic smart hybrid nanocomposite rupture trapezoidal plates subjected to yawed flow using DQHFEM, *Aerospace Science and Technology*, Vol. 145, pp. 108862, 2024.

[23] A. Tamrabet, B. Mamen, A. Menasria, A. Bouhadra, A. Tounsi, M. H. Ghazwani, A. Alnujaie, S. Mahmoud, Buckling behaviors of FG porous sandwich plates with metallic foam cores resting on elastic foundation, *Structural Engineering and Mechanics, An Int'l Journal*, Vol. 85, No. 3, pp. 289-304, 2023.

[24] A. A. Daikh, A. M. Zenkour, Effect of porosity on the bending analysis of various functionally graded sandwich plates, *Materials Research Express*, Vol. 6, No. 6, pp. 065703, 2019.

[25] D. Shahsavari, M. Shahsavari, L. Li, B. Karami, A novel quasi-3D hyperbolic theory for free vibration of FG plates with porosities resting on Winkler/Pasternak/Kerr foundation, *Aerospace Science and Technology*, Vol. 72, pp. 134-149, 2018.

[26] N. Wattanasakulpong, V. Ungbhakorn, Linear and nonlinear vibration analysis of elastically restrained ends FGM beams with porosities, *Aerospace Science and Technology*, Vol. 32, No. 1, pp. 111-120, 2014/01/01/, 2014.

[27] A. Attia, A. A. Bousahla, A. Tounsi, S. R. Mahmoud, A. S. Alwabli, A refined four variable plate theory for thermoelastic analysis of FGM plates resting on variable elastic foundations, *Structural engineering and mechanics: An international journal*, Vol. 65, No. 4, pp. 453-464, 2018.

[28] M. Sobhy, Thermoelastic response of FGM plates with temperature-dependent properties resting on variable elastic foundations, *International Journal of Applied Mechanics*, Vol. 7, No. 06, pp. 1550082, 2015.

[29] S. Pradhan, T. Murmu, Thermo-mechanical vibration of FGM sandwich beam under variable elastic foundations using differential quadrature method, *Journal of Sound and Vibration*, Vol. 321, No. 1-2, pp. 342-362, 2009.

[30] S. Refrafi, A. A. Bousahla, A. Bouhadra, A. Menasria, F. Bourada, A. Tounsi, E. A. Bedia, S. Mahmoud, K. H. Benrahou, A. Tounsi, Effects of hygro-thermo-mechanical conditions on the buckling of FG sandwich plates resting on elastic foundations, *Computers and Concrete, an International Journal*, Vol. 25, No. 4, pp. 311-325, 2020.

[31] A. Tounsi, A. Bouhadra, A. A. Bousahla, S. Mahmoud, A new and simple HSDT for thermal stability analysis of FG sandwich plates, *Steel and Composite Structures, An International Journal*, Vol. 25, No. 2, pp. 157-175, 2017.

[32] F. Bourada, K. Amara, A. Tounsi, Buckling analysis of isotropic and orthotropic plates using a novel four variable refined plate theory, 2016.

[33] S. Merdaci, A. Tounsi, A. Bakora, A novel four variable refined plate theory for laminated composite plates, *Steel Compos. Struct*, Vol. 22, No. 4, pp. 713-732, 2016.

[34] N. Himeur, B. Mamen, S. Benguediab, A. Bouhadra, A. Menasria, B. Bouchouicha, F. Bourada, M. Benguediab, Coupled effect of variable Winkler–Pasternak foundations on bending behavior of FG plates exposed to several types of loading, *Steel and Composite Structures, An International Journal*, Vol. 44, No. 3, pp. 353-369, 2022.

[35] N. Zouatnia, L. Hadji, Effect of the micromechanical models on the bending of FGM beam using a new hyperbolic shear deformation theory, *Earthquakes and Structures*, Vol. 16, No. 2, pp. 177-183, 2019.

[36] A. F. Radwan, Effects of non-linear hygrothermal conditions on the buckling of FG sandwich plates resting on elastic foundations using a hyperbolic shear deformation theory, *Journal of Sandwich Structures & Materials*, Vol. 21, No. 1, pp. 289-319, 2019.

[37] A. Safa, L. Hadji, M. Bourada, N. Zouatnia, Thermal vibration analysis of FGM beams using an efficient shear deformation beam theory, *Earthq. Struct*, Vol. 17, No. 3, pp. 329-336, 2019.

[38] Ş. D. Akbaş, Vibration and static analysis of functionally graded porous plates, *Journal of Applied and Computational Mechanics*, Vol. 3, No. 3, pp. 199-207, 2017.

[39] M. Bourada, A. Tounsi, M. S. A. Houari, E. A. A. Bedia, A new four-variable refined plate theory for thermal buckling analysis of functionally graded sandwich plates, *Journal of Sandwich Structures & Materials*, Vol. 14, No. 1, pp. 5-33, 2012.

[40] M. Sekkal, B. Fahsi, A. Tounsi, S. Mahmoud, A new quasi-3D HSDT for buckling and vibration of FG plate, *Structural Engineering and Mechanics, An Int'l Journal*, Vol. 64, No. 6, pp. 737-749, 2017.

[41] H.-T. Thai, D.-H. Choi, An efficient and simple refined theory for buckling analysis of functionally graded plates, *Applied Mathematical Modelling,* Vol. 36, No. 3, pp. 1008-1022, 2012/03/01/, 2012.